Supplementary information

Catalysts of Water Oxidation and pH Sensors Based on Azo-conjugated Iridium/Rhodium Motifs

Wei-Bin Yu*, Qing-Ya He, Hua-Tian Shi, Yan Pan, and Xianwen Wei*

Analysis and Testing Central Facility, School of Chemistry and Chemical Engineering, Anhui University of Technology, Maanshan 243002, P.R.China.

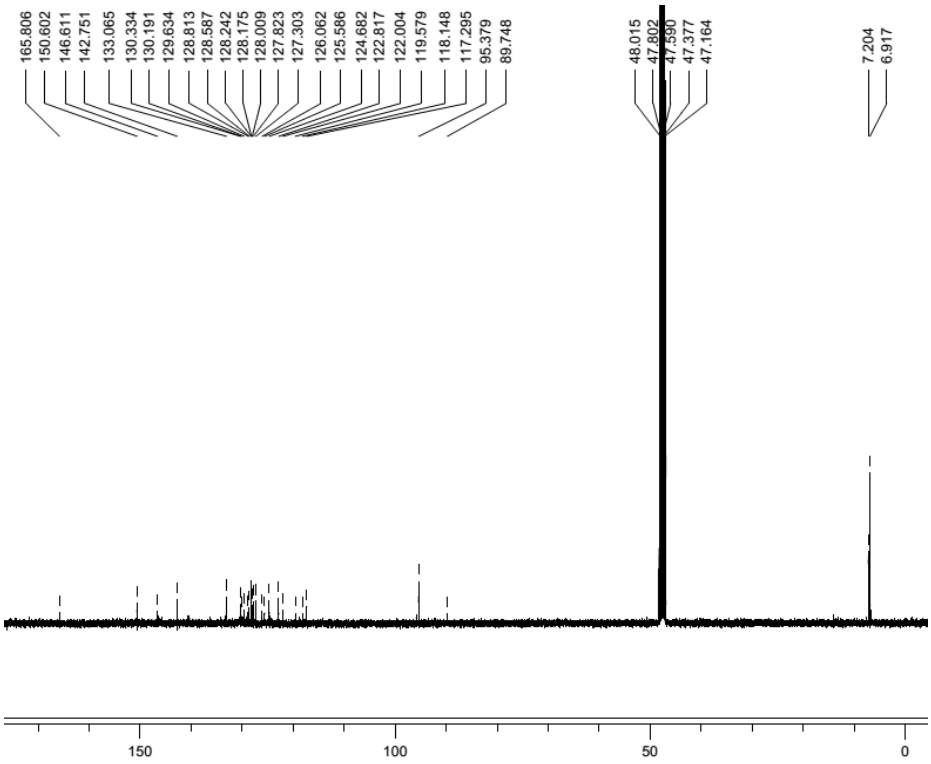

Figure s1. ^{13}C NMR spectra of **1**.

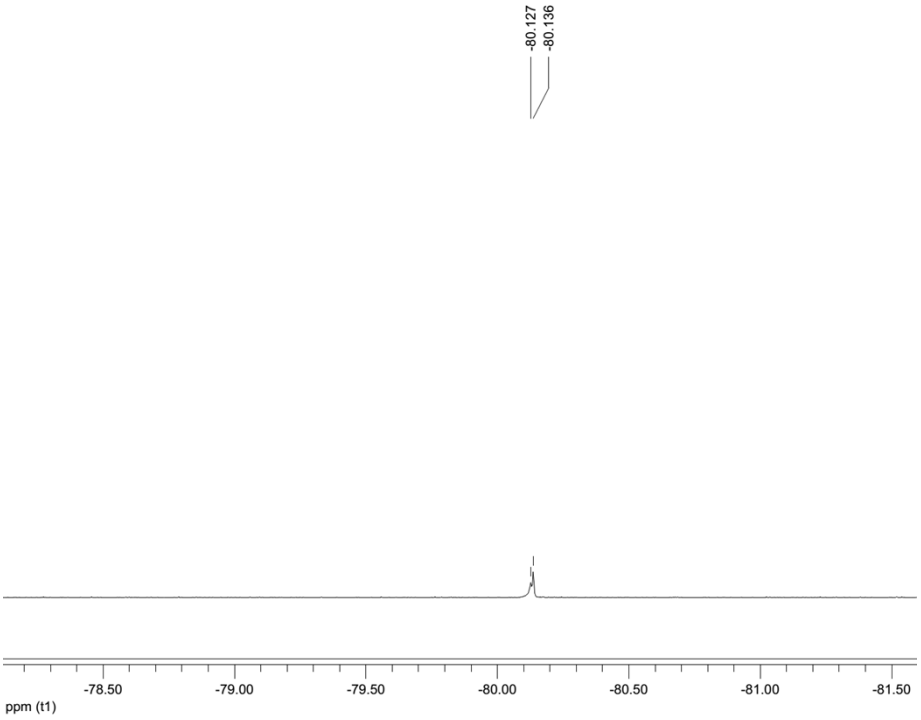

Figure s2. ^{19}F NMR spectra of **1**.

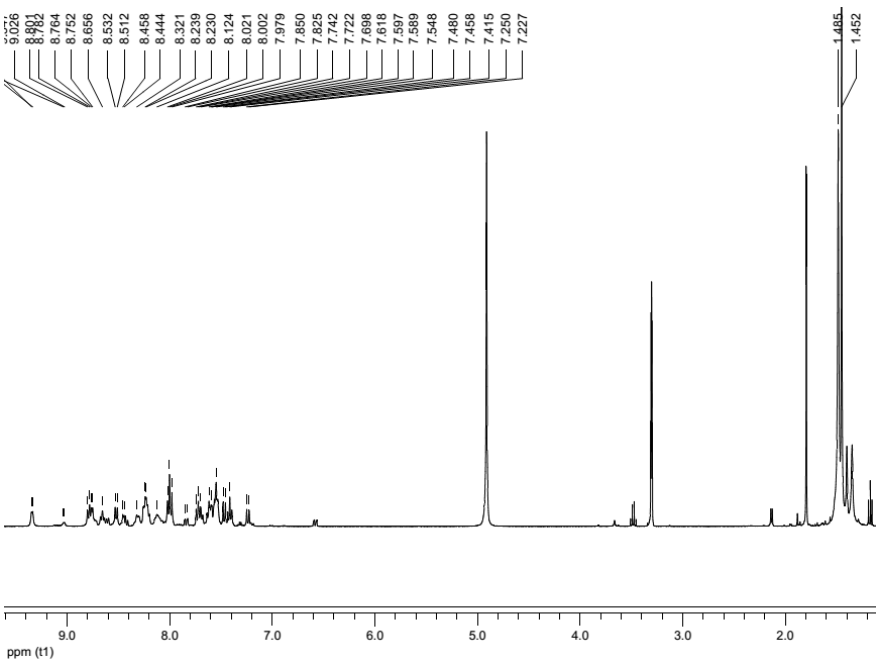

Figure s3. ^{1}H NMR spectra of **2**.

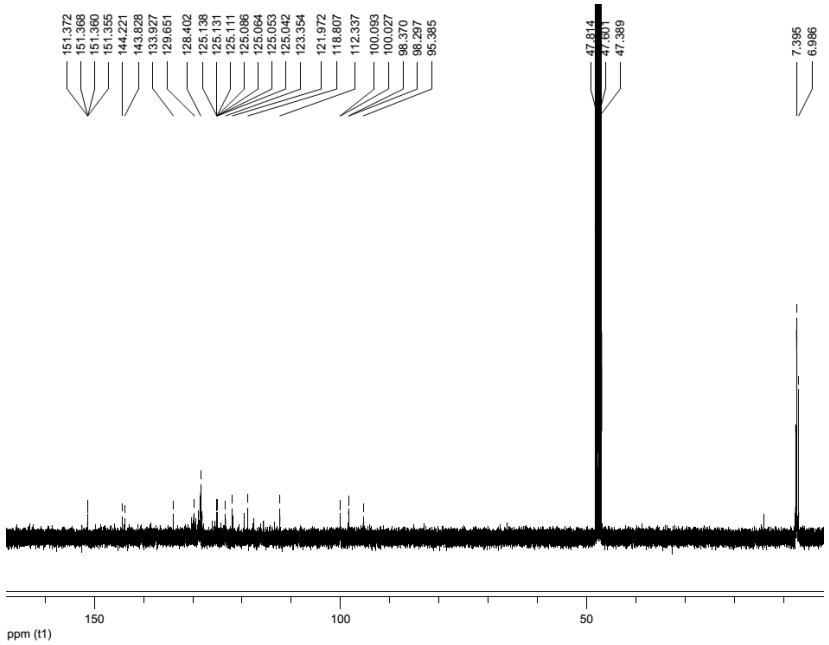

Figure s4. ^{13}C NMR spectra of **2**.

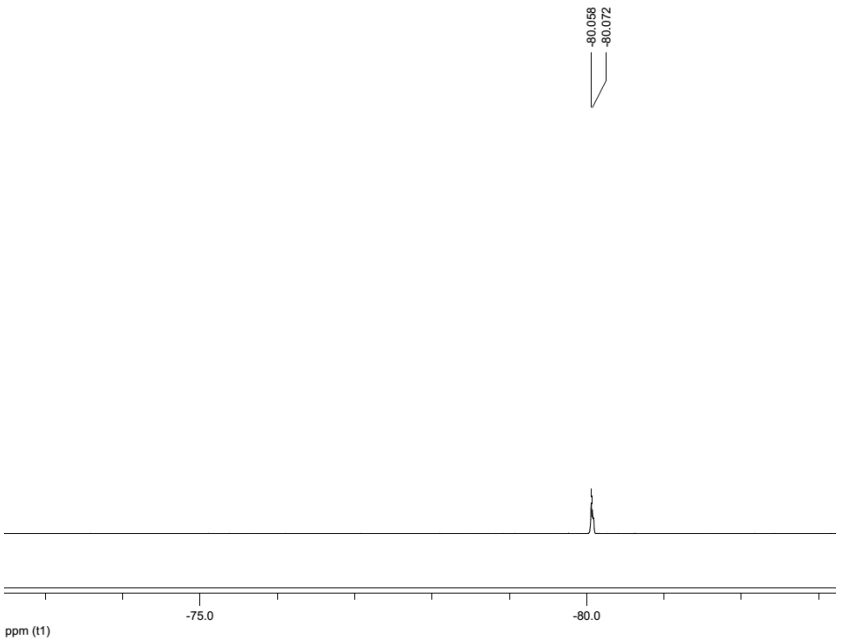

Figure s5. ^{19}F NMR spectra of **2**.

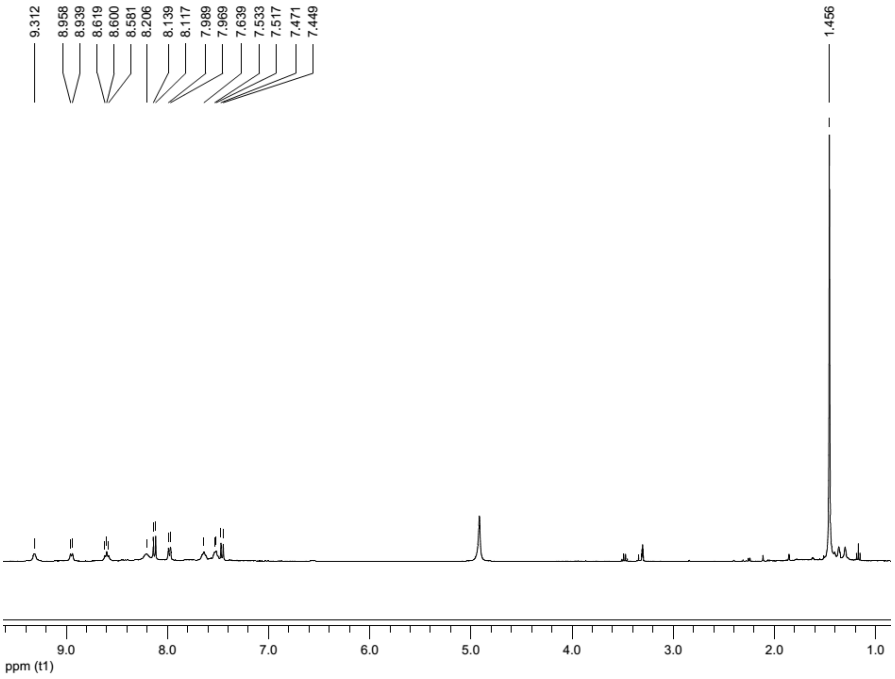

Figure s6. ^{1}H NMR spectra of **3**.

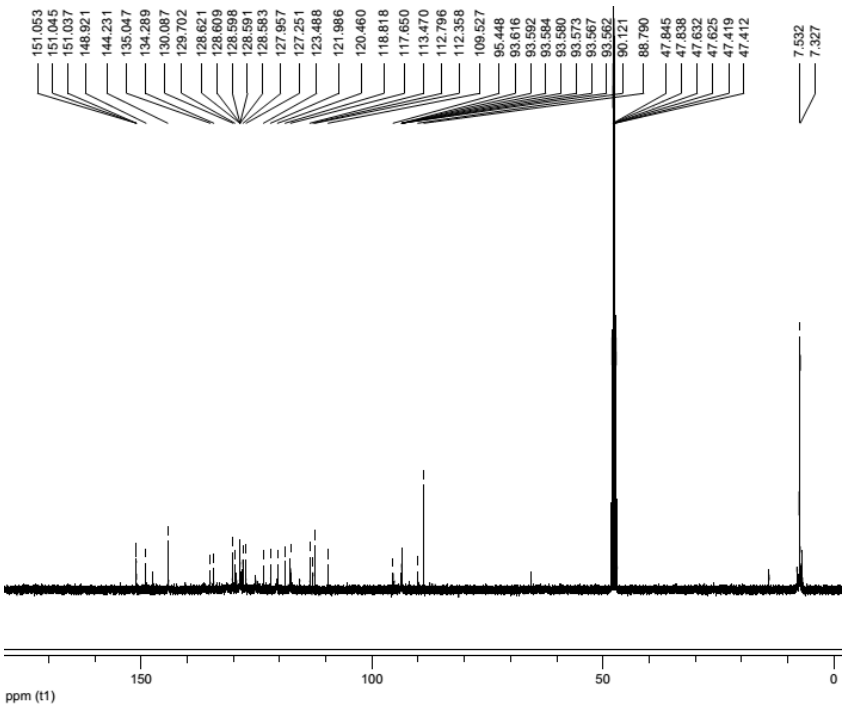

Figure s7. ^{13}C NMR spectra of **3**.

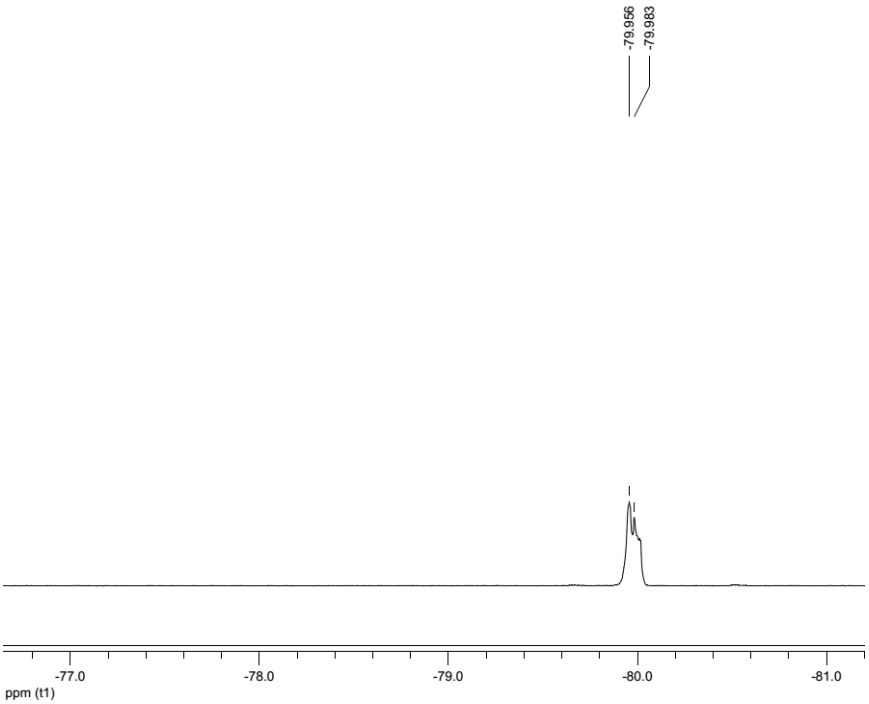

Figure s8. ^{19}F NMR spectra of **3**.

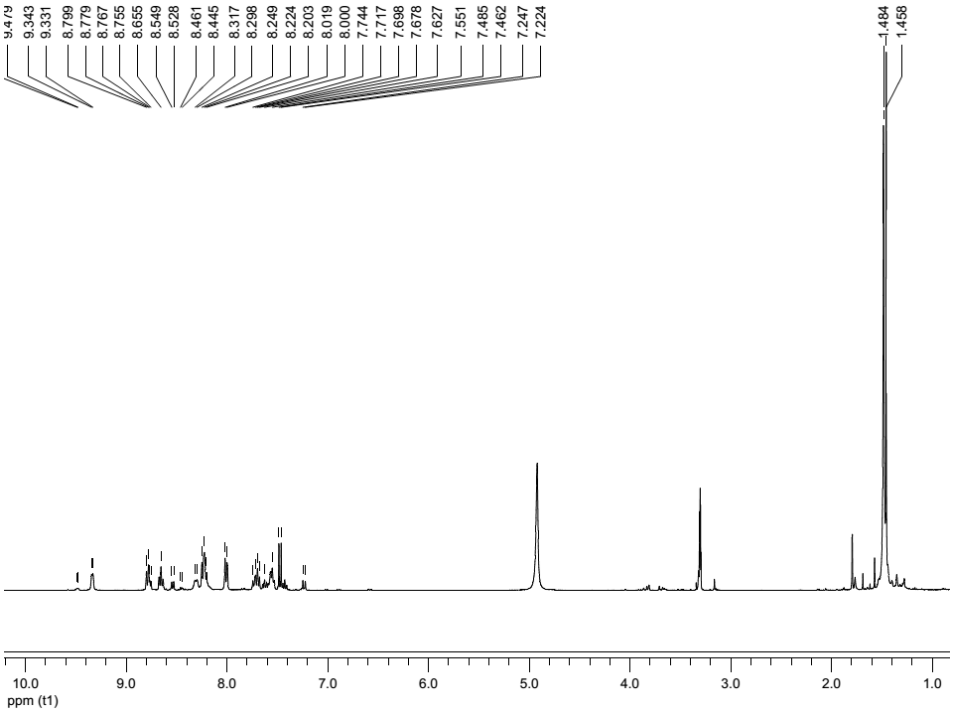

Figure s9. ^{1}H NMR spectra of **4**.

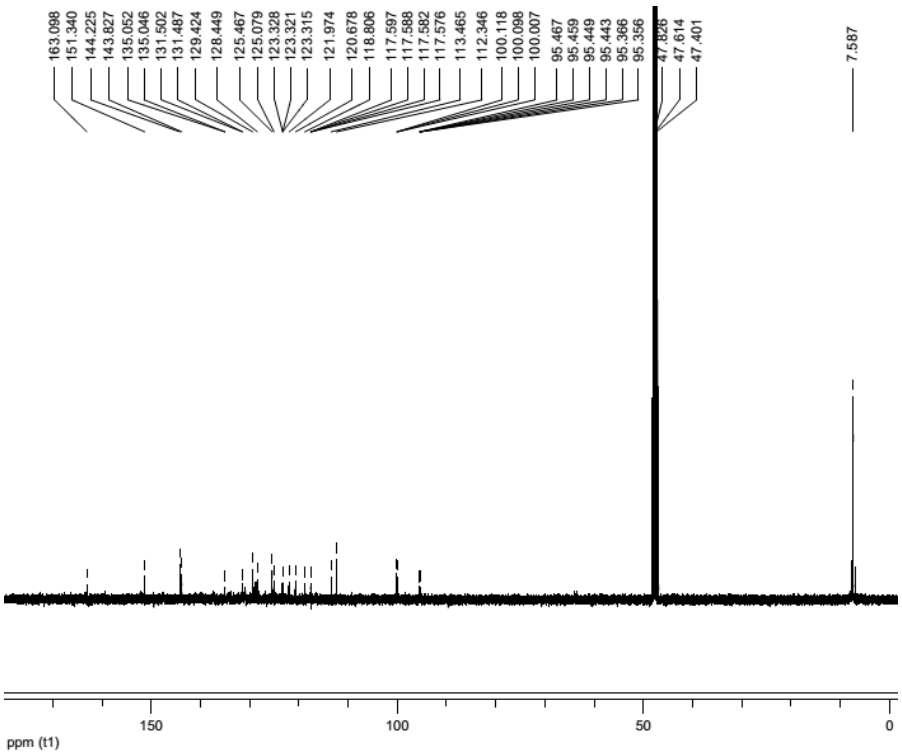

Figure s10. ^{13}C NMR spectra of **4**.

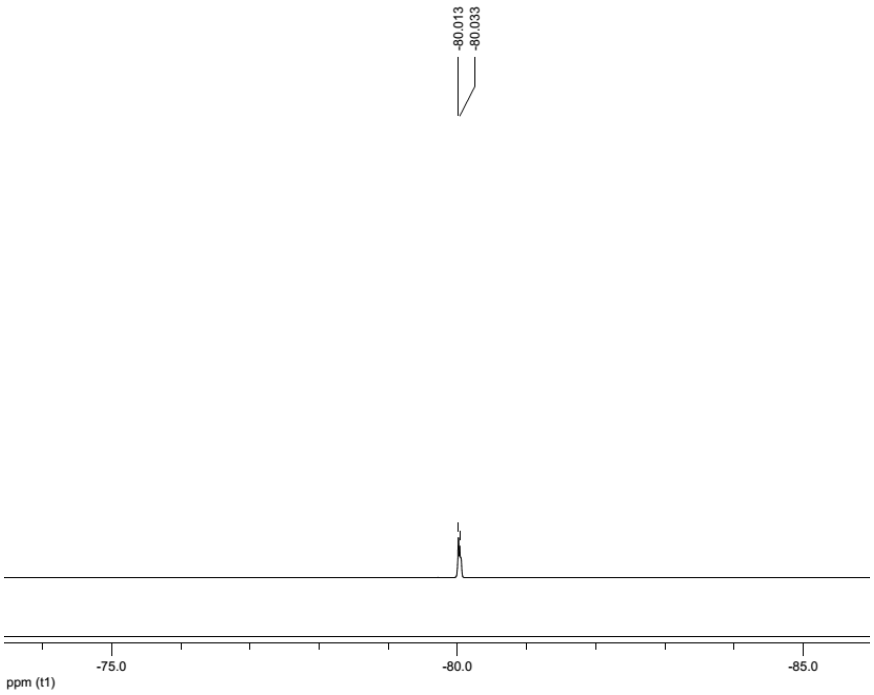

Figure s11. ^{19}F NMR spectra of **4**.

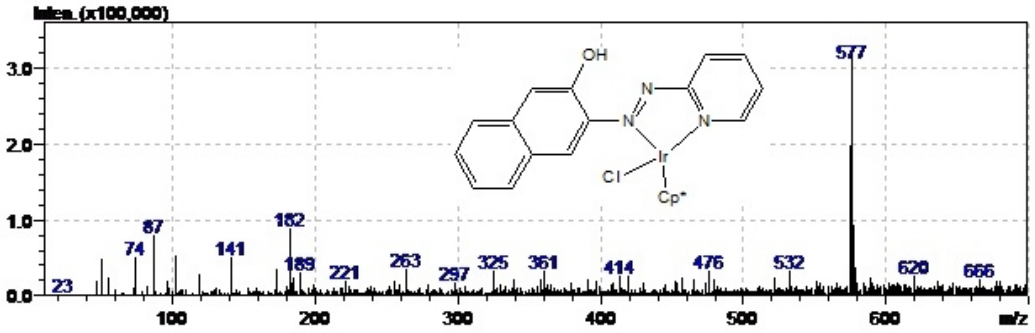

Figure s12. ESI-MS spectra of complex **1**.

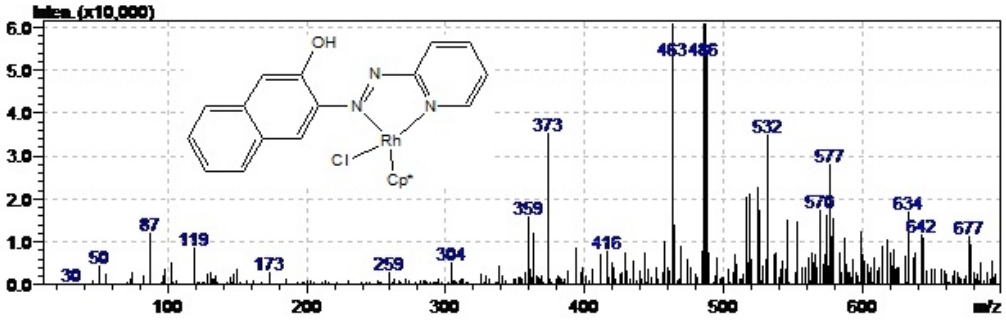

Figure s13. ESI-MS spectra of complex **2**.

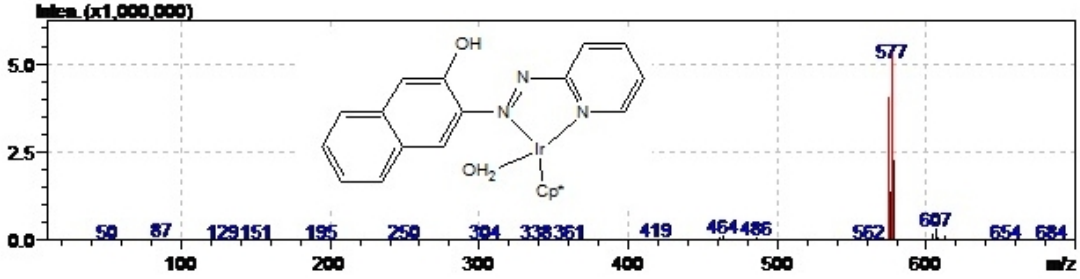

Figure s14. ESI-MS spectra of complex **3**.

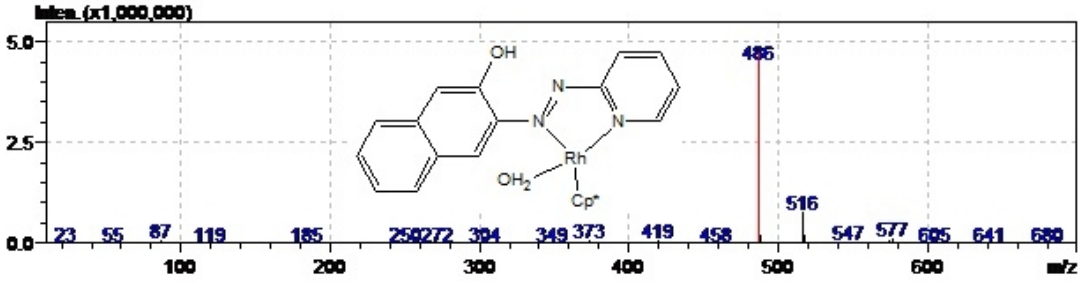

Figure s15. ESI-MS spectra of complex **4**.

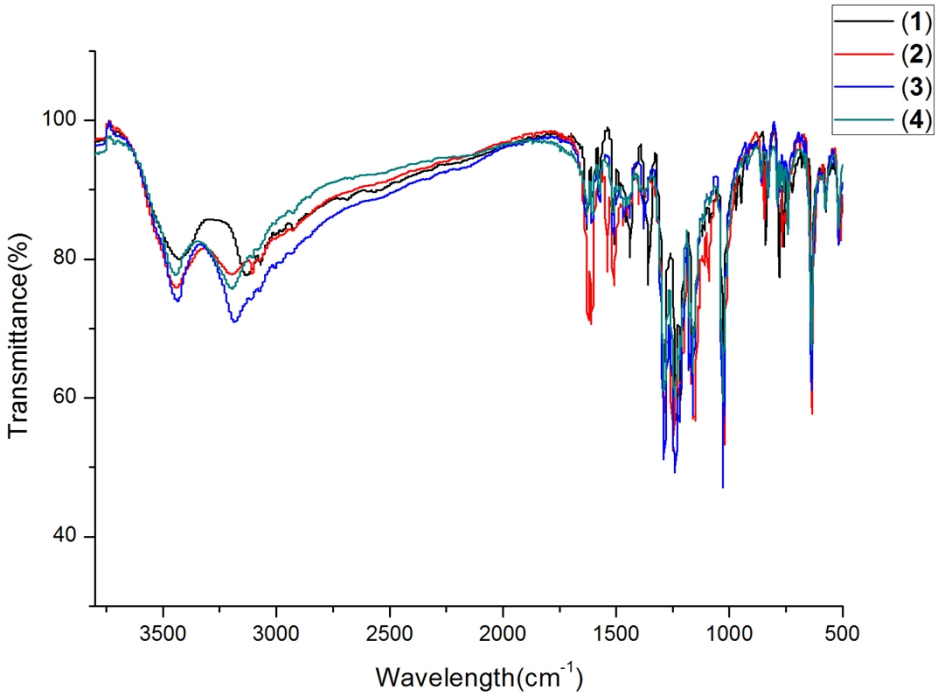

Figure s16. IR spectra of **1-4**.

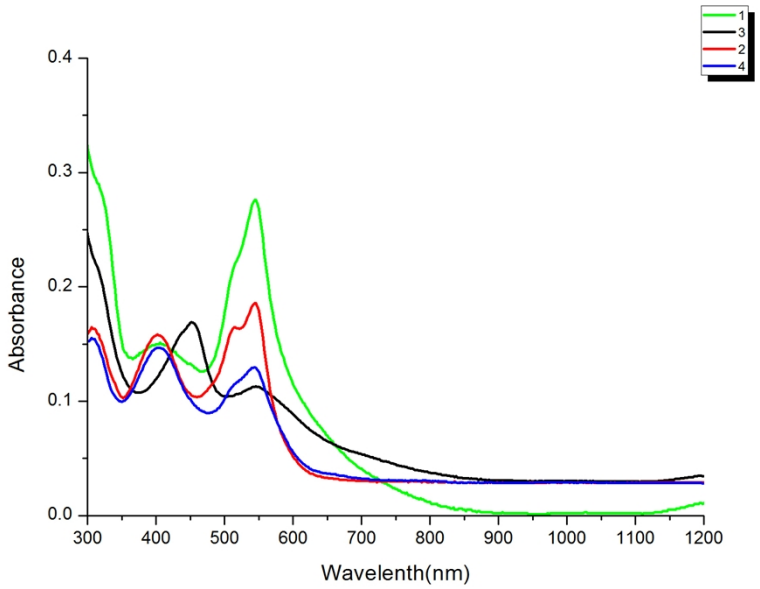

Figure s17. UV-Vis spectra of **1-4** in MeOH.

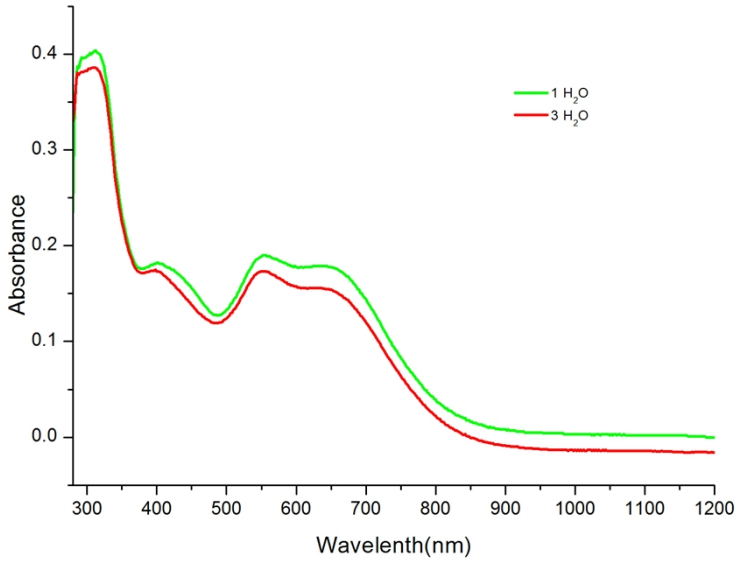

Figure s18. UV-Vis spectra of **1** and **3** in water.

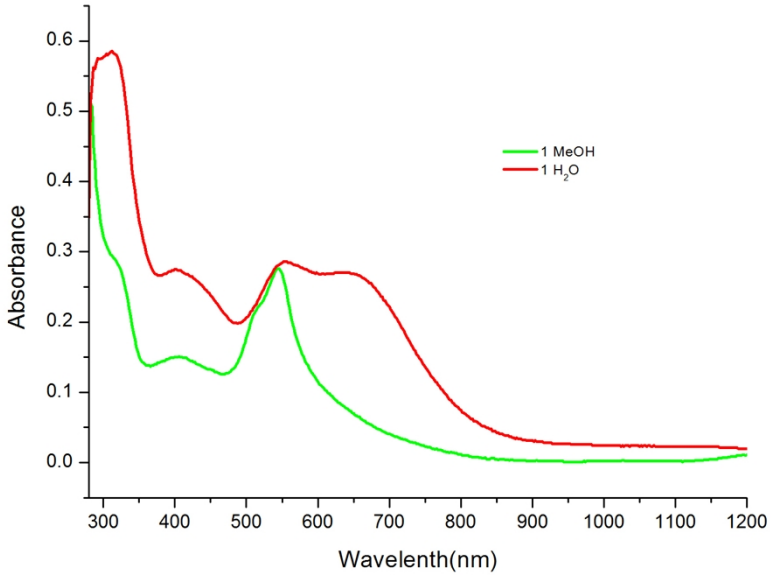

Figure s19. UV-Vis spectra of **1** in methanol and water.

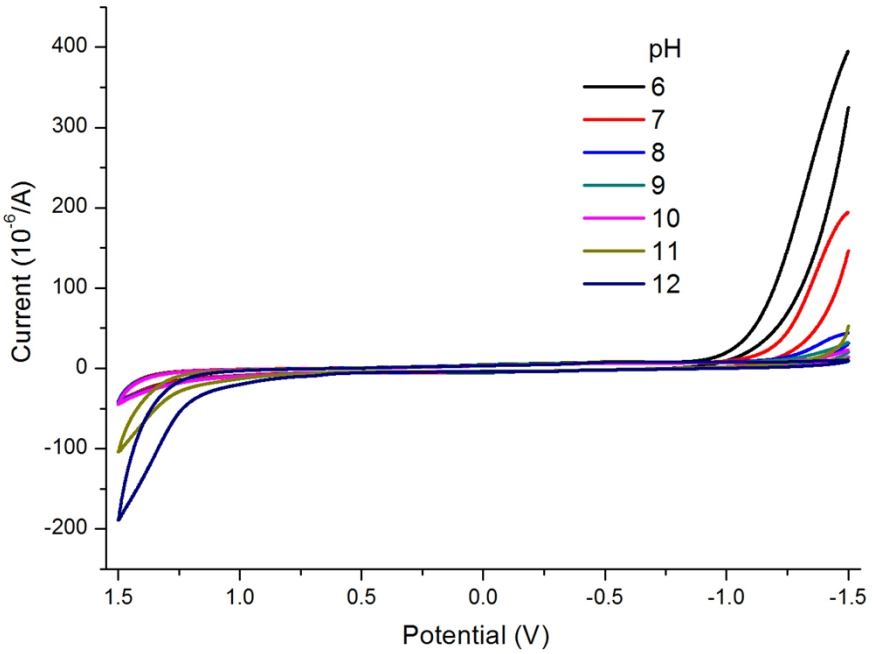

Figure s20. pH-dependent cyclic voltammograms of complex **2** in aqueous solution (Concentration: 0.03 mM, scan rate: 50 mV/s).

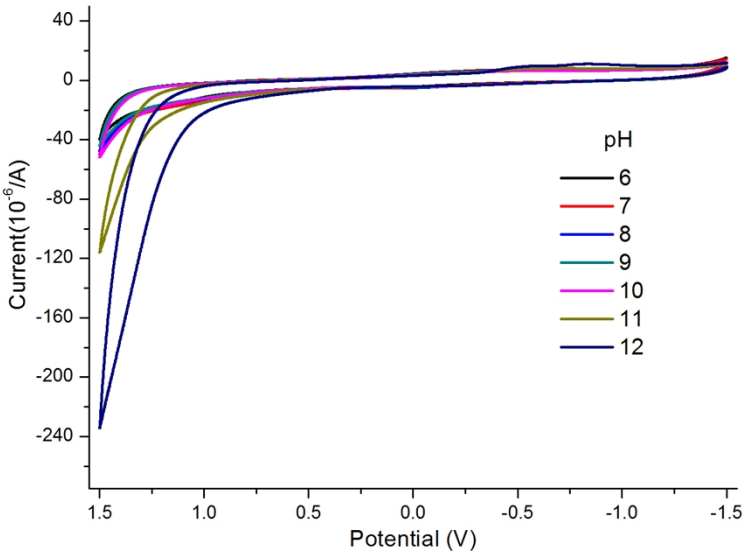

Figure s21. pH-dependent cyclic voltammograms of complex **3** in aqueous solution (Concentration: 0.03 mM, scan rate: 50 mV/s).

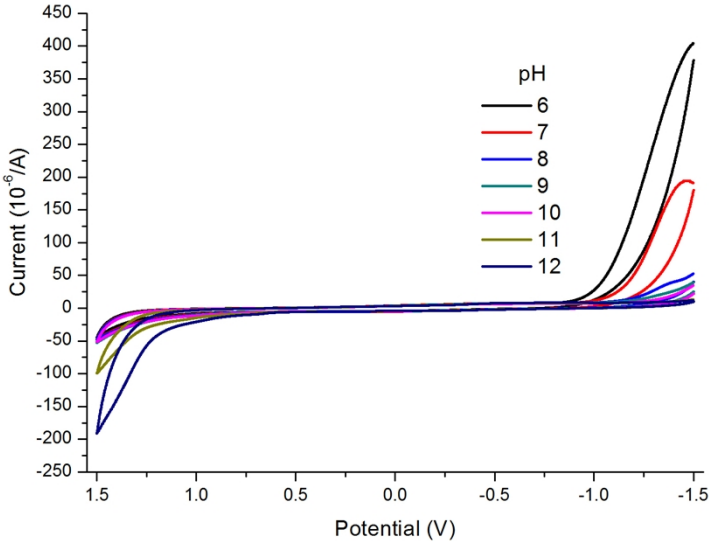

Figure s22. pH-dependent cyclic voltammograms of complex **4** in aqueous solution (Concentration: 0.03 mM, scan rate: 50 mV/s).

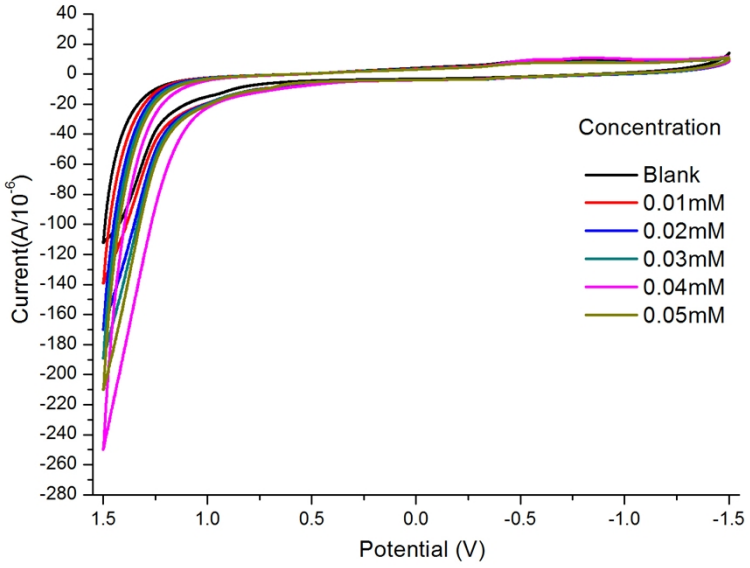

Figure s23. Concentration-dependent cyclic voltammograms of complex **2** in aqueous solution (pH = 12, scan rate: 50 mV/s).

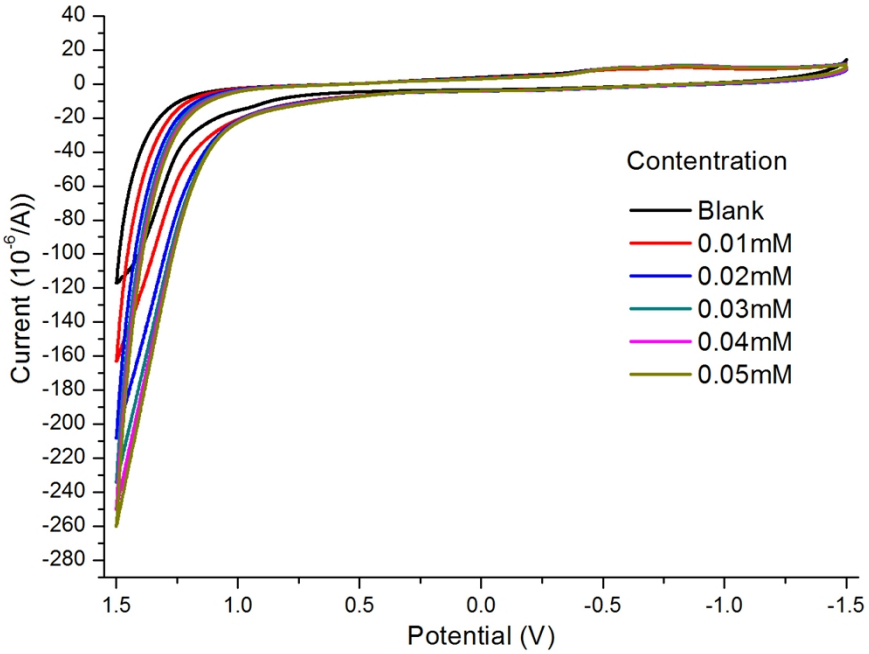

Figure s24. Concentration-dependent cyclic voltammograms of complex **3** in aqueous solution (pH = 12, scan rate: 50 mV/s).

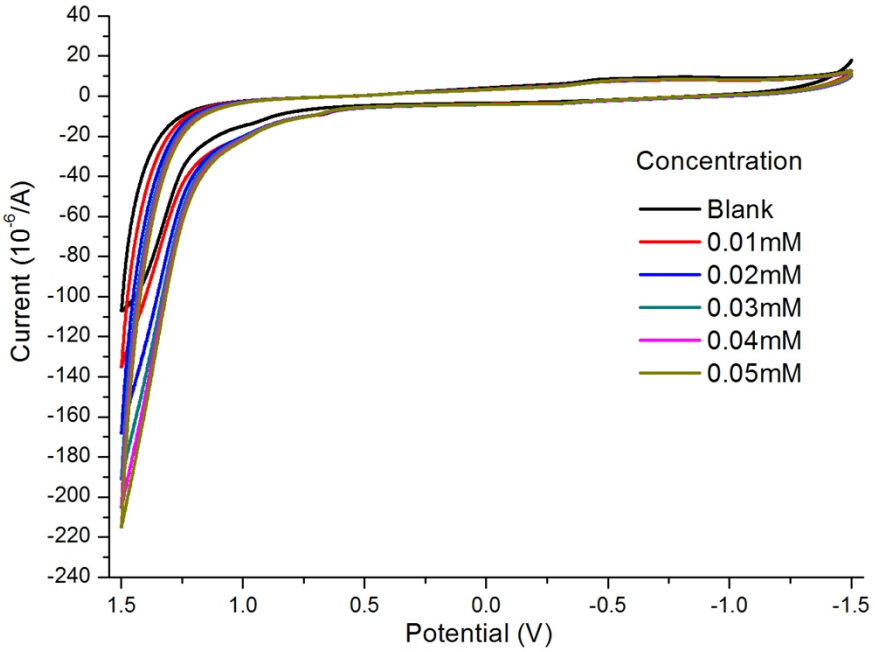

Figure s25. Concentration-dependent cyclic voltammograms of complex **4** in aqueous solution (pH = 12, scan rate: 50 mV/s).

Table s1. Crystal data and structure refinement for **2**.

Empirical formula	$C_{26}H_{26}ClF_3N_3O_4RhS$
Formula weight	671.92
Temperature	273(2) K
Wavelength	0.71073 A
Crystal system, space group	Monoclinic, P2(1)/c
Unit cell dimensions	a = 8.583(4) A alpha = 90 deg. b = 16.929(7) A beta = 99.892(5) deg. c = 19.659(8) A gamma = 90 deg.
Volume	2814(2) A^3
Z, Calculated density	4, 1.586 Mg/m^3
Absorption coefficient	0.833 mm^-1
F(000)	1360
Crystal size	0.25 x 0.15 x 0.10 mm
Theta range for data collection	2.41 to 27.71 deg.
Limiting indices	-11<=h<=11, -20<=k<=22, -17<=l<=25
Reflections collected / unique	16910 / 6409 [R(int) = 0.1042]
Completeness to theta = 27.71	97.1 %
Max. and min. transmission	0.9214 and 0.8188
Refinement method	Full-matrix least-squares on F^2
Data / restraints / parameters	6409 / 370 / 358
Goodness-of-fit on F^2	0.970
Final R indices [I>2sigma(I)]	R1 = 0.0813, wR2 = 0.1528
R indices (all data)	R indices (all data)
Largest diff. peak and hole	1.194 and -0.759 e.A^-3

Table s2. Crystal data and structure refinement for **3**.

Empirical formula	$C_{27}H_{26}F_6IrN_3O_8S_2$
Formula weight	890.83
Temperature	296(2) K
Wavelength	0.71073 A
Crystal system, space group	Triclinic, P-1
Unit cell dimensions	a = 9.205(2) A alpha = 102.389(3) deg. b = 11.366(3) A beta = 96.745(3) deg. c = 16.818(4) A gamma = 104.938(2) deg.
Volume	1632.4(6) A^3
Z, Calculated density	2, 1.812 Mg/m^3
Absorption coefficient	4.303 mm^-1
F(000)	872
Crystal size	0.24 x 0.20 x 0.15 mm
Theta range for data collection	2.52 to 27.48 deg.
Limiting indices	-11<=h<=11, -14<=k<=14, -15<=l<=21
Reflections collected / unique	10170 / 7188 [R(int) = 0.0213]
Completeness to theta = 27.48	96.2 %
Absorption correction	Semi-empirical from equivalents
Max. and min. transmission	0.5646 and 0.4249
Refinement method	Full-matrix least-squares on F^2
Data / restraints / parameters	7188 / 425 / 430
Goodness-of-fit on F^2	1.024
Final R indices [I>2sigma(I)]	R1 = 0.0429, wR2 = 0.1101
R indices (all data)	R1 = 0.0528, wR2 = 0.1155
Largest diff. peak and hole	2.382 and -1.602 e.A^-3

Table s3. Crystal data and structure refinement for **4**.

Empirical formula	$C_{27}H_{27}F6N_3O_8RhS_2$
Formula weight	802.55
Temperature	296(2) K
Wavelength	0.71073 A
Crystal system, space group	Triclinic, P-1
Unit cell dimensions	a = 9.1279(17) A alpha = 102.330(3) deg. b = 11.394(2) A beta = 96.882(2) deg. c = 16.825(3) A gamma = 104.537(2) deg.
Volume	1626.8(5) A^3
Z, Calculated density	2, 1.638 Mg/m^3
Absorption coefficient	0.739 mm^-1
F(000)	810
Crystal size	0.25 x 0.20 x 0.15 mm
Theta range for data collection	2.45 to 25.00 deg.
Limiting indices	-10<=h<=10, -13<=k<=10, -17<=l<=20
Reflections collected / unique	7914 / 5503 [R(int) = 0.0309]
Completeness to theta = 25.00	95.9 %
Max. and min. transmission	0.8973 and 0.8368
Refinement method	Full-matrix least-squares on F^2
Data / restraints / parameters	5503 / 431 / 431
Goodness-of-fit on F^2	1.055
Final R indices [I>2sigma(I)]	R1 = 0.0962, wR2 = 0.2134
R indices (all data)	R1 = 0.1343, wR2 = 0.2546
Largest diff. peak and hole	2.062 and -1.927 e.A^-3

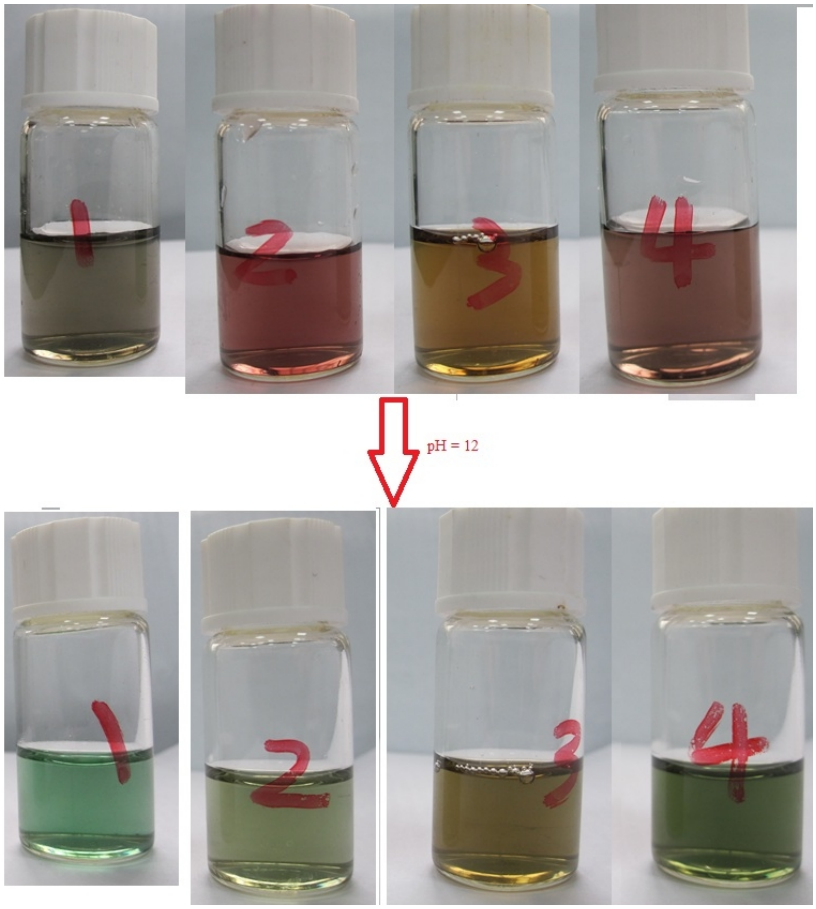

Figure s26. The transformation of color in complexes **1-4**.

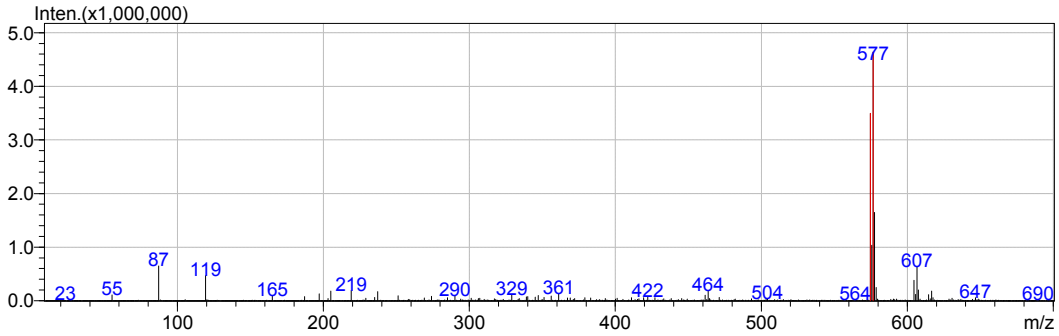

Figure s27. ESI-MS spectra of complex **1** at pH = 12.

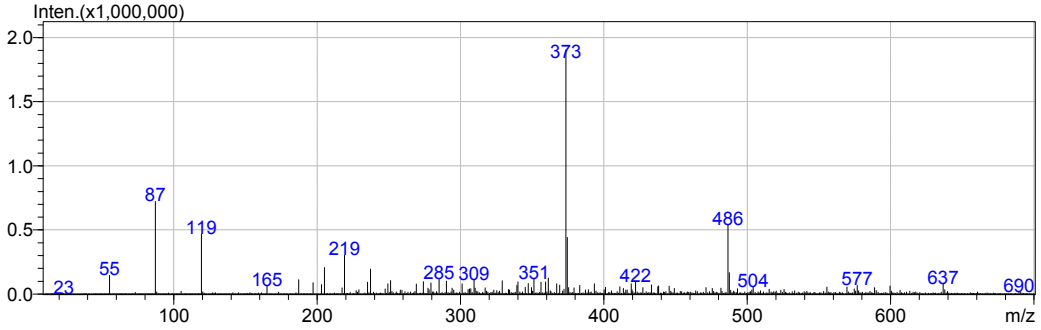

Figure s28. ESI-MS spectra of complex **2** at pH = 12.

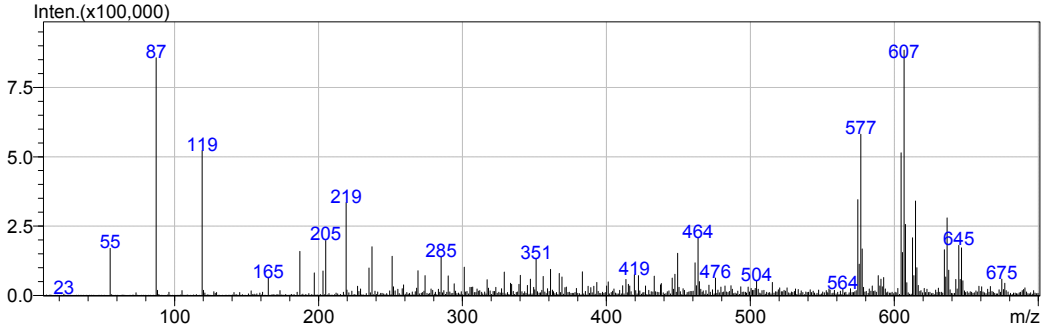

Figure s29. ESI-MS spectra of complex **3** at pH = 12.

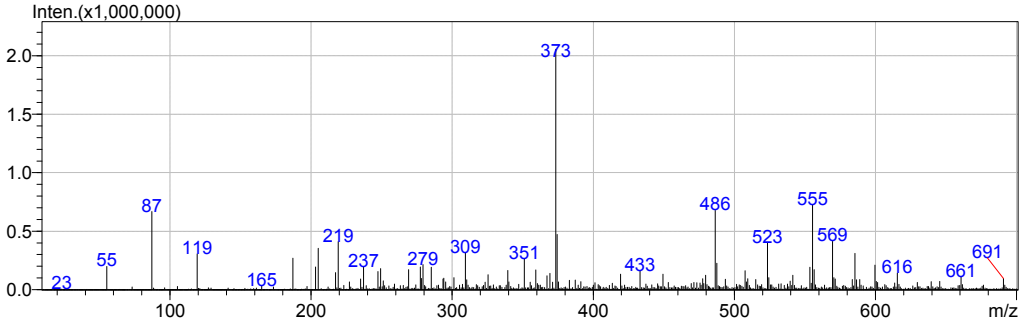

Figure s30. ESI-MS spectra of complex**4** at pH = 12.